Role of sandstone provenance in the diagenetic albitization of feldspars A case study of the Jurassic Tera Group sandstones (Cameros Basin, NE Spain)

Laura González-Acebrón [a,*], José Arribas [b], Ramón Mas [a]

[a] Dto. Estratigrafía, Facultad de Ciencias Geológicas (UCM), Instituto de Geología Económica (CSIC), C/Jose Antonio Novais 2, 28040 Madrid Spain
[b] Dto. Petrología y Geoquímica, Facultad de Ciencias Geológicas (UCM), Instituto de Geología Económica (CSIC), C/Jose Antonio Novais 2, 28040 Madrid, Spain

Keywords:
Albitization
K-feldspar
Plagioclase
Cathodoluminescence
Sandstone provenance

A B S T R A C T

The Cameros Basin (Iberian Chain, NE Spain) formed during the latest Jurassic–Early Cretaceous rifting stage in an extensional regime characterized by high subsidence rates. Its sedimentary infill (thicker than 6000 m) has been subdivided into eight depositional sequences (DS) mainly composed of continental sediments. DS 1 and DS 2 represent the first rifting stage (Tera Group, Tithonian), mainly formed by fluvial and lacustrine sediments. Sandstone petrofacies evolved from quartz-sedimentolithic in DS 1 to quartz-feldspathic in DS 2 due to the rifting process. In DS 2, three different types of detrital feldspars (K-feldspars, albites and polysynthetic plagioclases) with similar sodium-rich compositions (mean: $Ab_{94.0}$ $An_{4.5}$ albites (Ab>99%) are common. In DS 2, diagenetic albitization of both plagioclases and K-feldspars is inferred from conventional microscopy observations, cathodoluminescence and electron microprobe analyses. DS 1 contains few plagioclase grains, which show no evidence of transformation into albite. Although the albitization is characterized as diagenetic it seems to be provenance-controlled since it affects the units showing higher original plagioclase/K-feldspar ratio (DS 2), due to the greater influence of plutonic and metamorphic source areas in DS 2. Possible Na sources are: (1) the percolation of moderate to high salinity residual brines from related alkaline lakes developed at top of DS 2 in the eastern sector of the basin, (2) clay mineral reactions (sodium smectite to illite and chlorite) indicated by mudstone composition in the interlayered mudstones, and (3) the replacement of detrital sodium plagioclases by carbonate. These three sources can be complementary.

1. Introduction

The albitization of detrital K-feldspar and plagioclase is one of the most significant changes occuring in sandstones (McBride, 1985; Morad, 1988; Milliken, 2005) and this phenomenon considerably hinders provenance interpretations. When albitization takes place, the grain shape of the parent feldspar or plagioclase is preserved.

Albitization of K-feldspars and plagioclase can significantly alter the original sandstone framework composition to form several diagenetic products, such as calcite, kaolinite, dickite and illite, and may thus modify pore size and geometry (Boles, 1982; Saigal et al., 1988; Morad et al., 1990, 2000). Thus, identifying diagenetic albitization is essential for petrographic studies on sandstones. Moreover, low-grade metamorphic rocks sometimes contain sodium-rich feldspars (Trevena and Nash, 1981) and is often difficult to distinguish detrital grains from the authigenic albites.

Albitization affects both calcium–plagioclase grains (e.g. Boles, 1982; Gold, 1987; Morad et al., 1990; Ramseyer et al., 1992) and K-feldspar grains (e.g. Walker, 1984; Morad, 1988; Saigal et al., 1988; Aagaard et al., 1990), though the albitization of K-feldspars usually requires a greater burial depth (Morad et al., 1990) compared to plagioclase albitization.

In this paper, we characterize and interpret the albitization of detrital K-feldspars and plagioclases in the Tithonian sandstones of the Tera Group of the Cameros Basin (NE Spain, Fig. 1) as diagenetic but provenance-related. The Tera Group of the Cameros Basin is an excellent geological setting to explore the effects of the amounts and presence of detrital plagioclase and K-feldspars on albitization versus the absence of albitized feldspars. The possible controls of hydrothermal metamorphism on albitization are also discussed.

2. Geological setting

The Cameros Basin in the northern Iberian Range (Fig. 1) forms part of the Mesozoic Iberian Rift System (Mas et al., 1993; Guimerà et al., 1995; Salas et al., 2001; Mas et al., 2002). Intraplate rifting was a consequence of a generalized extensional regime that separated Iberia from Europe.

The Cameros Basin formed during the second rift event of the Iberian Rift, from the Tithonian to the early Albian. The basin-fill succession of the Cameros Basin embodies a large cycle or megasequence composed of up to 6000 m of sediments at the depocentre. This sedimentary infill has been divided into eight depositional sequences (Mas et al., 2002, 2003) and consists mainly of continental sediments corresponding to alluvial and

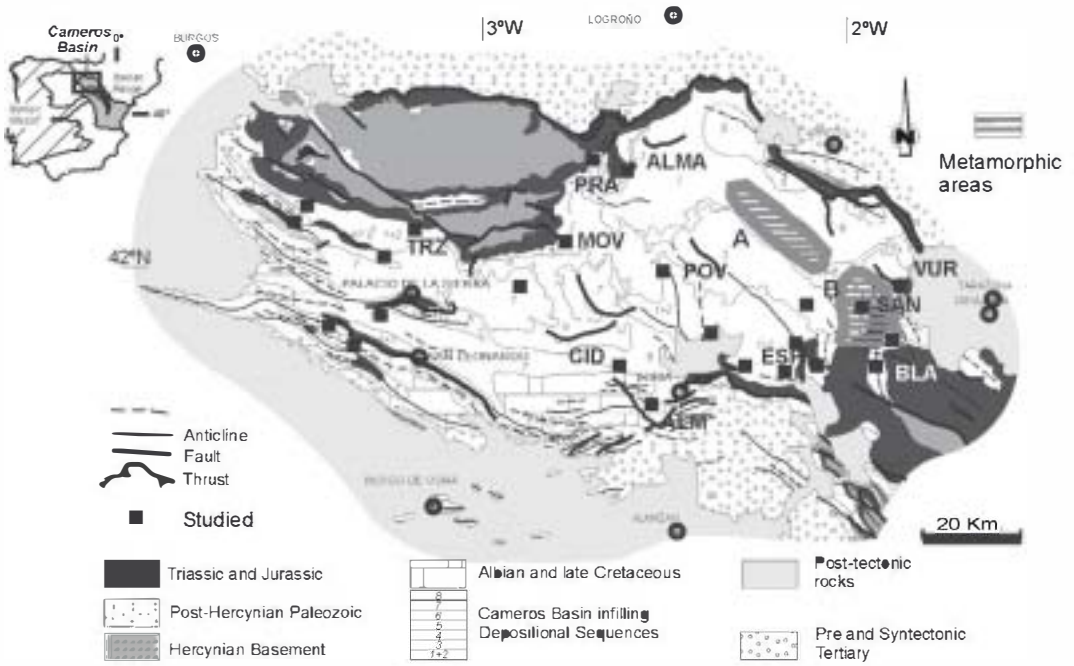

Fig. 1. Geological map of the Cameros Basin showing the areas affected by metamorphism (A and B). The position of the stratigraphic sections of the Tera Group is marked. The western sections of the basin have been studied by Arribas et al. (2003). MAG: Magaña. CSP: Collado de San Pedro. SAN: San Felices. AGE: Ágreda. VUR: Valdegutur, ESP: El Espino, BLA: San Blas, ALM: Almajano, POV: La Póveda, MOV: Montenegro de Cameros. CID: Cidones. TRZ: Terrazas. Shallow alkaline lakes were located in the southern part of the eastern sector of the basin (sections of MAG, CSP, SAN, AGE, VUR, Fig. 1). Modified by Mas et al. (2002).

lacustrine systems with scarce marine incursions (Mas et al., 1993; Gómez Fernández and Meléndez, 1994). The Tera Group represents the first stage of rifting sedimentation and comprises two depositional sequences (DS 1 and DS 2) dated as Tithonian (Mas et al., 1993; Martín Closas and Alonso Millán, 1998; Mas et al., 2004). The thickness and lateral continuity of DS 1 is highly variable, with a maximum thickness of 255 m close to the locality of San Blas (BLA, Fig. 1). This depositional sequence is represented by clastic alluvial facies and lacustrine–palustrine carbonate facies (Ágreda Fm.). DS 2 is especially thick, up to 1500 m at the depocentre (San Felices, SAN, Fig. 1), and consists of fluvial facies that grade upwards and laterally to carbonate lacustrine facies (Magaña and Sierra de Matute Fms.). These lakes evolve from shallow carbonate lakes to shallow alkaline ephemeral lakes with the presence of lenticular gypsum (González-Acebrón, 2009). These shallow alkaline lakes were located in the southern part of the eastern sector of the basin (Sierra de Matute Fm., sections of MAG, CSP, SAN, AGE, VUR, Fig. 1).

2.1. Siliciclastic deposits: provenance and diagenesis

As in other rifted basins (Evans, 1990; Garzanti et al., 2001, 2003), sandstone petrofacies indicate erosion of the pre-rift sedimentary substratum as rifting commenced, and erosion of the basement in later stages (González-Acebrón et al., 2007a) to give rise to a provenance cycle in a rifted basin, that is, the typical provenance evolution in this kind of basin (Arribas et al., 2007).

Main source areas inferred for the eastern sector of DS 1 were sedimentary units of the Mesozoic cover (carbonates and siliciclastics), metamorphic areas which probably correspond to the West Asturian Leonese Zone (WALZ) and the granites of the Central Iberian Zone (CIZ) at the top of DS 1 (González-Acebrón et al., 2010). Source areas for the eastern sector of SD 2 were low-grade to medium-grade metamorphic terranes (WALZ) and the granites of the CIZ, which presented higher influence in DS 2, showed lower influence of the sedimentary units (González-Acebrón et al., 2007a, 2010). In general, the evolution of the western sector (Arribas et al., 2003) is equivalent to the one of the eastern sector, but no plutonic rock fragments have been observed (González-Acebrón et al., 2010), and the detrital P/K index (plagioclase/K-feldspars) of DS 2 is lower in the western sector than in the eastern one (0.75 < 1.44, Arribas et al., 2003; González-Acebrón et al., 2010).

The diagenesis of the siliciclastic deposits of the Tera Group is revealed by different processes and cements, which have totally occluded the original porosity. The porosity of the sandstones (predominantly subarkoses) was reduced mainly by compaction (ICOMPACT = 0.78–0.95). This index decreases to the north of the eastern sector of the basin. The main processes and products of eodiagenesis are: a nonferroan and euhedral meteoric calcite, the start of mechanical compaction, K-feldspar replacement by kaolin and kaolin cements and K-feldspar cements (González-Acebrón, 2009).

During mesodiagenesis different generations of quartz cement precipitated, with homogenization temperatures (Th) of primary fluid inclusions between 114 and 141 °C (González-Acebrón et al., 2007b). Other mesodiagenetic phases are kaolin replacement by illite, ferroan calcite cement and albite cement. Chemical compaction continues throughout mesodiagenesis.

Telodiagenesis of the Tera Group deposits is related to the Alpine orogeny. Meteoric waters entered the system, with subsequent calcitization of ankerite and precipitation of carbonate cements in fractures (González-Acebrón, 2009).

The sedimentary record of the eastern sector of the Cameros Basin was affected by a hydrothermal event during the Late Albian to the Coniacian. Metamorphic conditions range from very low-grade (anchizone) to low-grade (epizone), with temperatures of 350–370 °C at the metamorphic peak and a maximum pressure of 1 Kbar (e.g. Casquet et al., 1992; Barrenechea et al., 1995). Saddle ankerite, pyrite, quartz and chlorite cements and replacements were generated during this hydrothermal process.

3. Sampling and methods

Samples of medium-grained sandstones were collected from 15 representative stratigraphic sections of the eastern sector of the Tera Group, and nine sections of the western sector (see Fig. 1 for locations).

Sections in the western zone have been sampled for a provenance study by Arribas et al. (2003). Doubly polished thin (30 μm) sections were prepared for both sectors. After a cathodoluminescence (CL) study, these thin sections were etched and stained using HF and sodium cobaltinitrite for potassium feldspar identification (Chayes, 1952). The CL study was performed using a cold cathodoluminescence instrument (Citl MK4, conditions: 300–500 μA, 11–16 kV and 0.1–0.2 Torr). For the microanalytical tests, we used a Jeol JXA-8900 M microprobe with four detectors under the working conditions: 15 kV, 20 nA and 5 μm of diameter of the electron beam. Measured oxides were CaO, Na_2O and K_2O, and mean detection limits were 290, 300 and 225 ppm for each element.

Doubly polished thin sections were prepared without heating and glued to frosted glass with cyanoacrylate for the fluid inclusion study. After petrographic analysis (conventional microscopy), selected areas of the thin sections were cut and removed from the glass backing in acetone. These portions of samples were examined on a Linkam THMSG-600 stage. Accurate measurements were only possible in four fluid inclusions due to their very small size (1–4 μm). Homogenization temperatures (Th) were interpreted as minimum entrapment temperatures. No pressure corrections were applied because a pressure determination would involve too many error-prone assumptions (Goldstein and Reynolds, 1994).

4. Results

Three different types of feldspars were identified under conventional microscopy in the eastern sector of the Cameros Basin: (1) untwinned, turbid K-feldspars or plagioclases (Fig. 2A); (2) untwinned bright rectangular plagioclases riddled with fluid inclusions (Fig. 2B); and (3) polysynthetic twinned plagioclases, also showing fluid inclusions (Fig. 2C).

Type 1 feldspar in DS 1 is stained with sodium cobaltinitrite usually as large grains (0.25 mm), whereas similar, finer grained (0.15 mm) feldspars in DS 2 do not take up the stain. Thus in DS 1, type 1 is K-feldspar (mean composition: Or_{98}) but presents a plagioclase composition in DS 2 (mean composition: $Ab_{96\ 1}\ An_{3.1}\ Or_{0.8}$). In addition, the type 1 feldspar shows K-feldspar overgrowth (10–20 μm thick) in DS 1 and albite overgrowth in DS 2 of equivalent thickness. Finally, type 1 K-feldspar includes microcline in DS 1 (Fig. 2D), but it is not observed in DS 2.

Types 2 and 3 feldspars are closely associated with each other and only appear in DS 2. Both types are non-stainable and show albite composition (mean composition: $Ab_{94\ 0}\ An_{4.5}\ Or_{1.5}$) and chemically pure albite overgrowths (Ab>99%, 15–40 μm thick). These types are riddled with primary fluids inclusions, mainly all-liquid, displaying elongated shapes parallel to the long axis of the plagioclase. Around 20% of the fluid inclusions feature a gas bubble, with liquid to vapour ratios between 95:5 and 85:15. These fluid inclusions are 2–6 μm in size. Homogenization temperatures of cogenetic fluid inclusion assemblages (FIAs) in albitized plagioclases (types 2 and 3) are 83–115 °C and are consistent (more than 90% of the fluid inclusion in the fluid inclusion assemblage homogenizing within 10–15 °C, Goldstein and Reynolds, 1994). Final melting temperatures of ice are between −16.9 and −20.1 °C. The relicts of detrital plagioclase grains were avoided in fluid inclusion measurements. Finally, type 3 grains commonly exhibit optical continuity between polysynthetic twinning of the grain and overgrowth.

Microprobe analysis of feldspar grains in the eastern sector reveals K-feldspar composition in DS 1 (mean composition: $Ab_{1.4}\ An_{0.1}\ Or_{98.5}$), and similar sodium-rich composition of the three feldspar types in DS 2 (mean composition: $Ab_{94.0}\ An_{4.5}\ Or_{1.5}$). In detail, in the lower DS 2 (Magaña Fm.), 85% of the feldspars are albite (Ab 90–100%), 14% oligoclases (Ab 70–90%) and 1% andesine (Ab 65–70%). In addition, 32% of feldspars are chemically pure albite (Ab>99%). In the upper DS 2

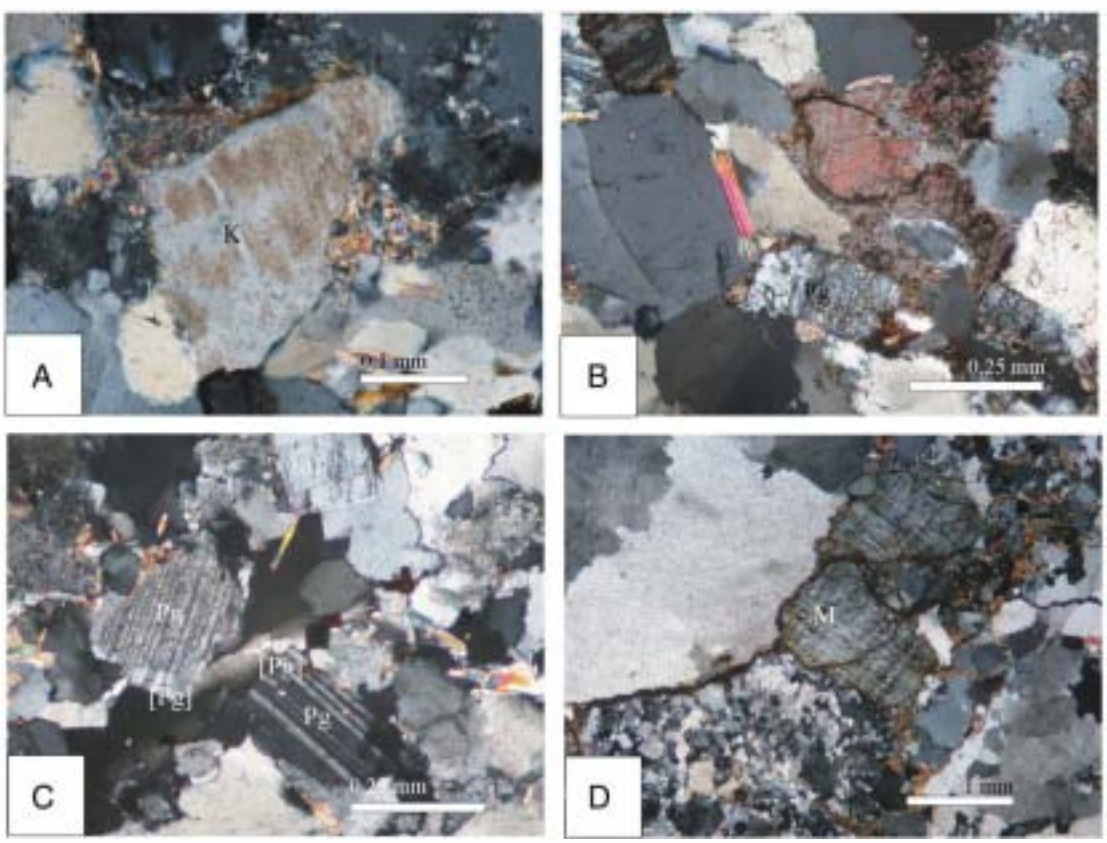

Fig. 2. Photomicrographs of the different types of feldspars in the Tera Group (crossed nichols): A. Albitized K-feldspar (K, type 1). DS 2. B. Albitized detrital albite (Pg, type 2). DS 2. C. Albitized polysynthetic plagioclase grain (Pg) showing well developed overgrowths (type 3). Note that cement twining ([Pg]) is optically continuous with grain twining. DS 2. D. Microcline (M, type 1). DS 1.

(Sierra de Matute Fm.), 77% of all feldspars are albite, 18% are oligoclase and 3% are andesine; 25% offeldspars being pure albite (Figs. 3, 4 and 5). Thus, K-feldspar is absent in the eastern sector of DS 2 and the three types show a plagioclase composition. Medium compositional values for DS 2 sections of the eastern sector with alkaline lacustrine deposits on top (south area, Fig. 1) are $Ab_{94.5}$ $An_{3.1}$ $Or_{2.4}$, whereas in the rest of the studied sections of the eastern sector the values are $Ab_{89.0}$ $An_{8.1}$ $Or_{2.9}$ (Appendixes 1 and 2).

In addition, K-feldspars in DS 1 (type 1) show blue luminescence (Fig. 6A and B). The type 1 plagioclases of albitic composition of DS 2 sandstones are usually nonluminescent or show very weak remains of blue luminescence (Fig. 6C and D). Nonluminescent areas are common in the fractured grains and on cleavage traces, generating parallel thin nonluminescent lines in this type of feldspar (Fig. 6E and F). Relicts of the blue luminescent sanidine (original composition before albitization) were detected in the type 1 plagioclases of DS 2 by backscattered electron imaging (BSE) and CL. These relicts feature linear shapes and sizes from 10 to 20 μm (Fig. 7A, B and C).

Types 2 and 3 plagioclases are nonluminescent yet in rare cases show green or blue luminescence (Figs. 6C, D, E, F; 7A, B, C, D, E, F). The higher the Ca content (up to 35%, Figs. 4 and 5) the more luminescentis the plagioclase, whereas albites are usually completely nonluminescent (Figs. 4 and 5). Some plagioclase grains show green and blue luminescence in the same grain (Fig. 7E and F), with compositional differences ranging from plagioclase to K-feldspar depending on the colour of the luminescence. Variations in cathodoluminescence related to polysynthetic twining are also observed (Fig. 7H). In type 3 plagioclases, backscattered electron imaging (BSE) and CL revealed very small andesine inclusions (10–20 μm) parallel to the polysynthetic twining (Fig. 7D).

In general, the three types of plagioclase grains in DS 2 are usually nonluminescent or show very weak luminescent remains. Nonluminescent plagioclases are represented close to the albite pole in Figs. 4A and 5, other compositions being uncommon. On the other hand, luminescent plagioclases usually present an albite composition, but andesines and oligoclases are also possible compositions. Thus, luminescent plagioclases display greater compositional dispersion.

Alteration processes differ in the three types of feldspars (González-Acebrón, 2009). Type 1 feldspar is replaced by kaolinite or illite. Illite replacement gives rise to the characteristic fan morphologies of the precursor kaolinite. Type 2 feldspar is partly replaced by illite. In type 3, unaltered and partly illitized plagioclases are closely associated with each other. Typical calcite replacement or cement may be seen in the immediate vicinity of sodium-rich plagioclase grains (type 3). This calcite presents a euhedral morphology, clear appearance, orange luminescence and no zonation.

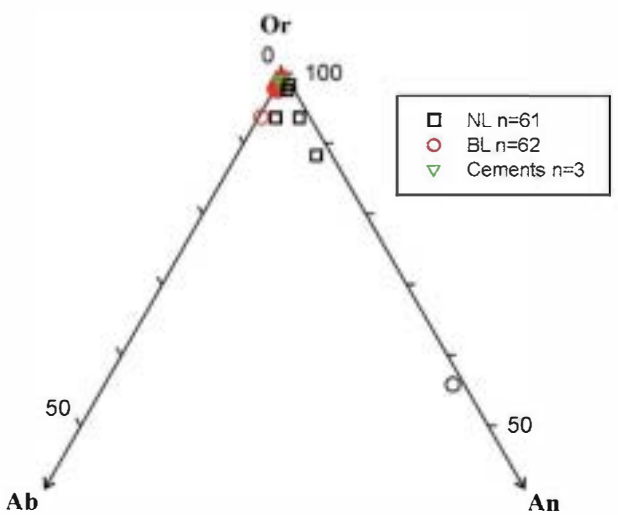

Fig. 3. Composition of the Ágreda Fm. (DS 1) non-albitized K-feldspars (type 1) in relation to their cathodoluminescence colour. NL: Nonluminescent. BL: Blue luminescent.

Similar types of feldspar are encountered in sandstones from DS 1 and DS 2 of the western sector of the Cameros Basin: K-feldspars of type 1 in DS 1 and the three types of plagioclases in DS 2. These three types are mostly of albitic composition (63% of albites, 29% showing very pure albite compositions: Ab>99%, Appendix A), but there are also type 1 non-albitized K-feldspars. Mean composition of all types of feldspars from DS 2 of this sector is $Ab_{77.0}$ $An_{2.9}$ $Or_{20.1}$ (Appendix A).

X-ray diffraction analysis of the interlayered mudstones (Tables 1 and 2) indicates the presence of feldspars (until 18%) with main reflexions at 3.19 and 3.21 Å, illite and chlorite as the most common clay minerals. Previous data of Barrenechea et al. (2001) determines a lower grade assemblage with the presence of mixed-layered smectite–illite ($R=1$, 65–85% illite layers) in the southern border of the basin (ALM, Fig. 1).

5. Discussion

5.1. Diagenetic albitization and provenance relationship

The three types of feldspar in the Tithonian–Berriasian sandstones (DS 2) of the rift start in the eastern sector of the Cameros Basin show a sodium-rich plagioclase composition (Ab: 65–100%). Based on the following evidence, this finding probably reflects a diagenetic albitization process:

1. The absence of detrital K-feldspar indicated by sodium cobaltinitrite staining and electron microprobe analysis.
2. The three morphological types of feldspar are very similar in composition (mean composition: $Ab_{94.0}$ $An_{4.5}$ $Or_{1.5}$) rich in sodium (Figs. 4B, 5B and 8), irrespective of textural type.
3. Chemically pure albite is relatively common ($Ab_{>99\%}$, Fig. 8). A purely albitic plagioclase composition is typical of diagenetic albite (e.g. Kastner, 1971; Boles, 1982; Walker, 1984; Saigal et al., 1988).
4. The lack of CL shown by most of the feldspar grains since diagenetically albitized feldspars are typically nonluminescent (e.g. Kastner, 1971; Saigal et al., 1988; Ramseyer et al., 1992). Nonluminescent grains are rich in albite and the higher their sodium contents, the lower the luminescence (Figs. 4A and 5A).
5. Cathodoluminescence shows evidence of partial albitization (Boles, 1982; Ramseyer et al., 1992; Caja, 2004; Ochoa, 2006). The greater compositional dispersion of luminescent plagioclase grains when compared to nonluminescent plagioclase grains (Figs. 4A and 5A, DS 2) could be the result of partial albitization of these luminescent grains, which preserve some weak blue or green luminescence (Fig. 6C and D). Partially blue or green luminescent grains with nonluminescent zones along microfractures or across cleavage planes also indicate partial albitization (Figs. 6E, F, 7A and B). However, in some plagioclase grains, different luminescence colours give rise to a zoned appearance (Fig. 7E and F). These are probably igneous-zoned grains, due to the higher melting point of anorthite versus albite, making the grain core richer in anorthite (Hurlbut and Klein, 1990).
6. Sanidine or andesine inclusions in types 1 and 3 plagioclases (respectively) of DS 2 can be interpreted as relicts of the original grain composition (Fig. 7A, B, C and D). Type 1 is interpreted as albitized detrital K-feldspars, based upon the sanidine composition of the relicts, the turbid appearance typical of K-feldspars (Fig. 2A), the characteristic untwinned grains and the remains of the original blue luminescent colour of K-feldspars (Figs. 6C, D, E, F, and 7A, B and C). No relicts were observed in type 2 plagioclase, which can be interpreted as albitized untwinned detrital plagioclase, according to its rectangular shape (Fig. 2B), bright appearance (Fig. 2B) and

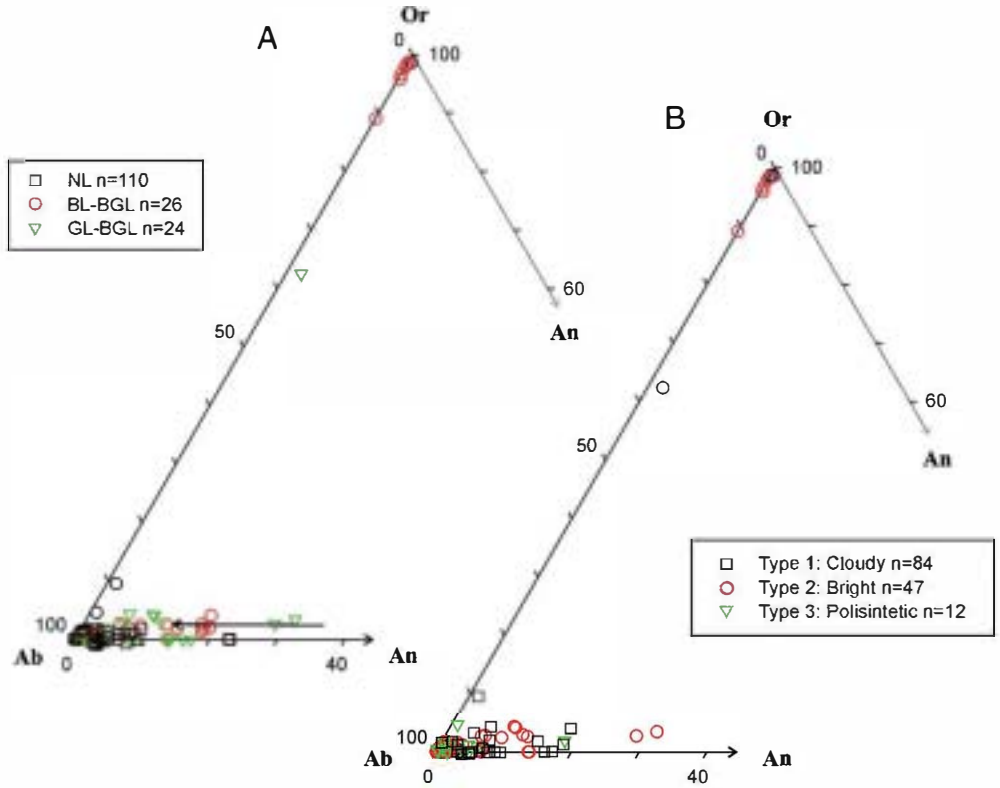

Fig. 4. Composition of the Magaña Fm. (DS 2) albitized K-feldspars and plagioclases in relation to their cathodoluminescence colour and feldspar type. NL: Nonluminescent. BL: Blue luminescent. BGL: Blue green luminescent. GL: Green luminescent. The feldspars close to the anorthite pole are either relict K-feldspars of partially albitized grains or non-albitized K-feldspars.

luminescence colours (nonluminescent or showing remains of green or blue, Fig. 6C, D, E, F). Type 3 is interpreted as albitized detrital polysynthetic plagioclase, as may be inferred from its bright appearance (Fig. 2C) and colours of luminescence (nonluminescent or showing remains of green or blue, Fig. 7A, B, G and H). In the grains in which relicts were recognized, type 3 exhibited an original andesine composition (Fig. 7D).

Feldspars in the DS 2 in the western sector of the basin usually present the same features than in the eastern sector with the exception of evidence 1 and 2, because the chemical composition of type 1 feldspars is sometimes K-feldspar and the mean composition of the three types is richer in K ($Ab_{77.0}$ $An_{2.9}$ $Or_{20.1}$, Appendix A) than in the eastern sector ($Ab_{94.0}$ $An_{4.5}$ $Or_{1.5}$, Appendix A). Thus, we deduce a lower intensity of the albitization process in the western sector compared to the eastern sector, which is reflected by the chemical composition of feldspars in the western sector, with only 63% of albites.

Another possible hypothesis is the albitization of DS 2 in both basin sectors were not diagenetic and occurred in the source rock, but no albitized units or sodium-rich feldspar units have been described in these areas. Although a sodium-rich unit could have existed and have been eroded, feldspars present several different source areas for DS 2 (probably CIZ and WALZ). In addition, type 1 feldspars are similar in both DS 1 and DS 2, but are only albitized in DS 2, pointing to a diagenetic process.

Diagenetic albitization of DS 1 would be expected since the albitization of K-feldspar is more likely at greater depths and temperatures (Morad

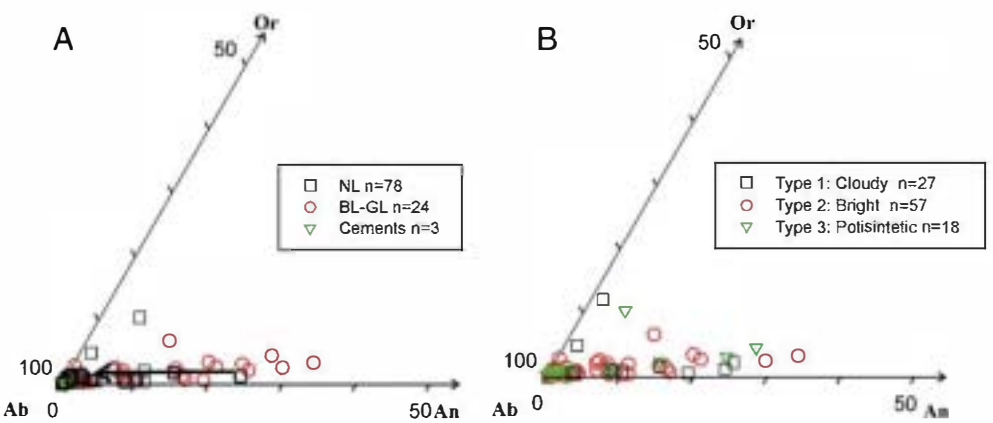

Fig. 5. Composition of the Sierra de Matute Fm. (DS 2) albitized K-feldspars and plagioclases in relation to their cathodoluminescence colour and feldspar type. NL: Non-luminescent. BL-GL: Blue or green luminescent. Relict K-feldspars not represented.

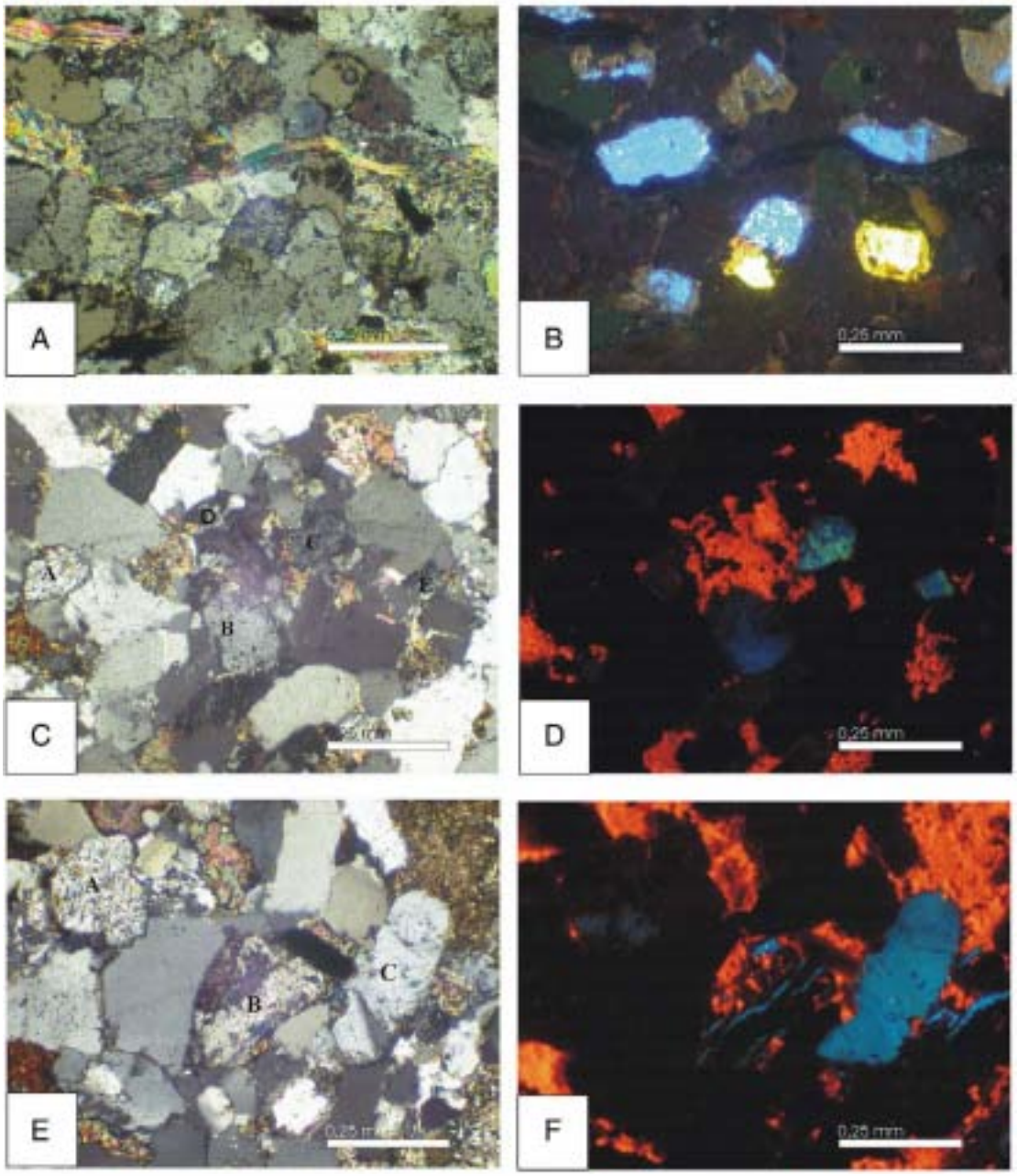

Fig. 6. Photomicrographs of the different types of feldspars in the Tera Group (crossed nichols and cathodoluminescence): A and B: Type 1 feldspars of potassium composition and intense blue luminescence. Yellow luminescent grains are apatites. DS 1. C and D: (A) Nonluminescent type 2 feldspar (detritic albite). (B) Albitized type 1 K-feldspar showing weak blue luminescence. Note the nonluminescent areas that grow from the edges to the centre of the grain. (C) Albitized type 1 feldspar showing blue and green luminescence. (D) Albitized type 2 feldspar (detritic albite), nonluminescent and partiallyreplaced by carbonate. (E) Albitized type 2 feldspar (detritic albite) showing green and blue zonation. E and F: (A) Albitized type 2 feldspar (detritic albite) with remains ofits original blue luminescence. (B) Albitized type 1 feldspar partiallyreplaced by carbonate Nonluminescent areas follow the cleavage planes. (C) Albitized type 1-feldspar showing blue luminescence.

et al., 1990). As has been explained, the source areas for the two DS were different, with signs of a greater influence of plutonic and metamorphic areas in DS 2 and probably different plutonic source rock compositions (González-Acebrón et al., 2007a, 2010). In DS 1, plutonic source areas probably present a potassium-rich composition, whereas a mixed potassium and calcium–sodium composition has been interpreted for DS 2 (González-Acebrón et al., 2010), implying a clear increase of the P/K ratio in DS 2. A further line of evidence is the presence of microcline in DS 1. Neither microcline nor albite grains of chessboard texture (related to the albitization of microcline, Morad, 1988) has been observed in DS 2.

Given that DS 2 is rich in detrital plagioclases in the eastern sector of the basin (González-Acebrón et al., 2010), albitization is probably diagenetic but its spatial and temporal distribution is controlled by sandstone provenance. The lower albitization degree of the western

Fig. 7. A, B and C: Partially albitized detrital K-feldspars and plagioclases. Notice the relicts of sanidine with the original luminescent colour. D. Albitized plagioclase showing relicts of andesine. E and F: Plagioclase with zoned appearance. G and H: Partially albitized polysynthetic plagioclase. Microprobe compositions: Ab: albite. An: anortite. Or: ortose.

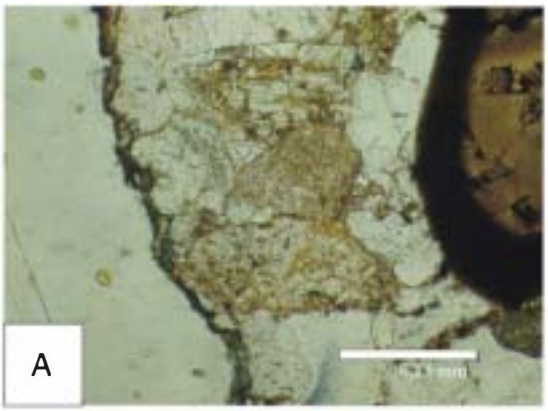

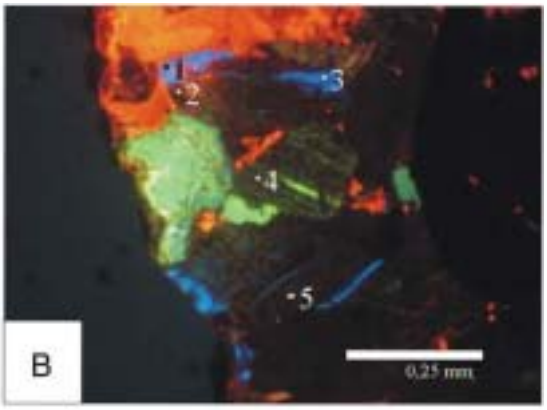

	[1]	[2]	[3]	[4]	[5]
Ab %	3,890	98,030	3,435	92,736	98,625
An %	0,319	0,335	0	4,024	0,282
Or %	95,790	1,635	96,565	3,241	1,093

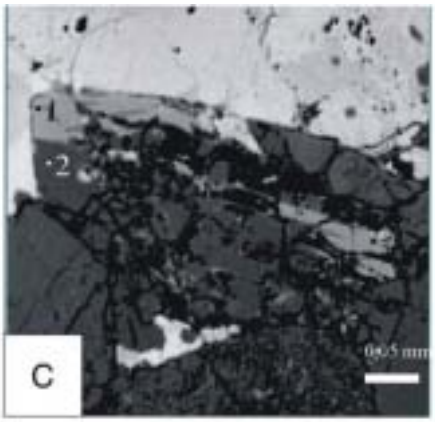

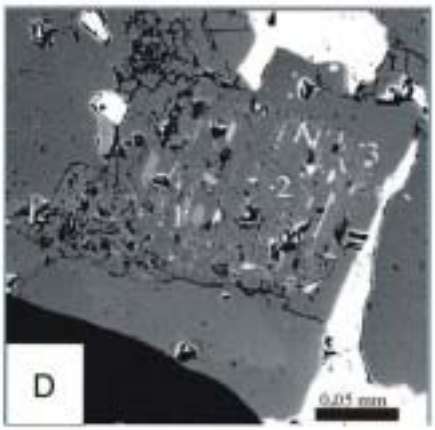

	[1]	[2]	[3]
Ab %	68,271	1,140	0,139
An %	31,501	95,852	99,557
Or %	0,227	3,009	0,745

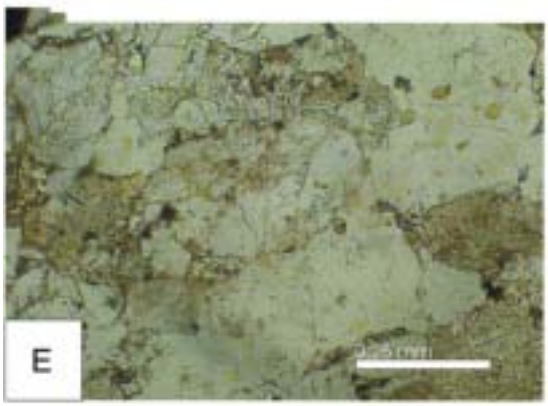

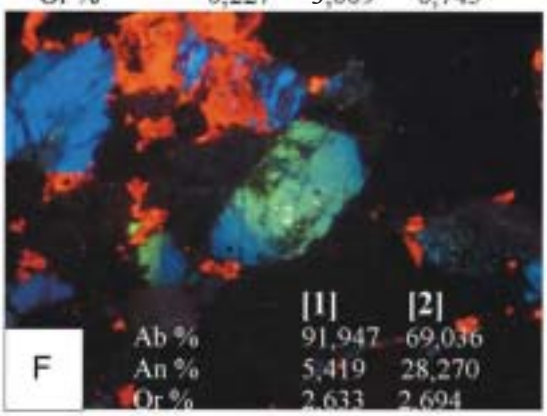

	[1]	[2]
Ab %	91,947	69,036
An %	5,419	28,270
Or %	2,633	2,694

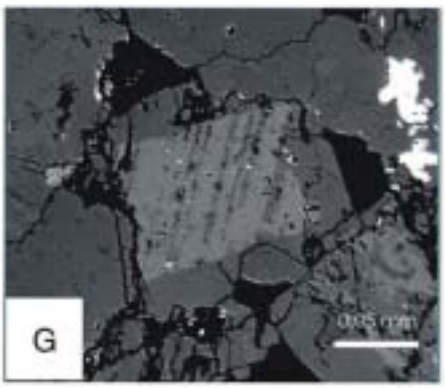

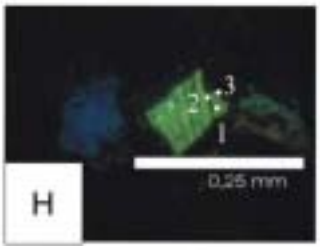

	[1]	[2]	[3]
Ab %	69,204	89,546	99,421
An %	26,327	9,532	0,538
Or %	4,469	0,921	0,041

Table 1
Semiquantitative percentage data for the main minerals detected by X-ray diffraction in the clay mudstones of the eastern sector of the Tera Group (DS 2). Interbedded mudstones contain feldspars (until 18%), which are probably mainly Ca–Na plagioclases due to the position of their main reflexions (3.19 and 3.21 Å). Stratigraphic sections: PRA: Pradillo, ALMA and ARZA: Almarza, SAN: San Felices, El Espino (ESP) and Valdegutur (VUR). Magaña: Magaña Fm. Matute: Sierra de Matute Fm.

Sample	Quartz	Dolomite	Calcite	Chlorite	Gypsum	Plag.	Phillos.	Fms.
PRA7	6	0	0	0	0	9	85	Magaña
ALMA3	100	0	0	0	0	0	0	Magaña
ALMA6	51	0	49	0	0	0	0	Magaña
ALMA8	6	0	23	59	0	12	0	Magaña
ALMA12	3	0	17	33	0	4	44	Magaña
ALMA15	10	0	50	28	0	12	0	Magaña
ARZA2	5	0	13	0	0	7	75	Matute
ARZA4	5	0	7	27	0	9	51	Matute
ARZA8	4	0	2	46	0	7	41	Matute
1SAN2	7	0	37	0	0	12	44	Ágreda
3SAN10	8	0	38	36	0	18	0	Magaña
3SAN11	5	0	17	13	0	10	56	Magaña
3SAN30	10	0	60	16	0	14	0	Matute
3SAN34	15	0	0	0	18	5	62	Matute
3SAN37	7	0	81	0	12	0	0	Matute
3SAN41	10	0	0	0	10	10	69	Matute
ESP101	6	0	0	0	0	0	94	Ágreda
ESP102	5	0	15	0	0	5	75	Magaña
VUR108	4	25	24	0	0	0	47	Magaña

sector can be related to the lower detrital P/K ratio of this sector compared to the eastern one (0.75>1.44).

Minimum entrapment temperatures of the albitization fluid are 83–115 °C. Necking down can be ruled out as a possible change after the entrapment of fluid inclusions in plagioclases on the basis of the consistent Th recorded in each FIA. Thus, primary all-liquid fluid inclusions are interpreted as metastable liquids, trapped above 50 °C showing no bubbles, probably due to problems of nucleation metastability (Goldstein and Reynolds, 1994). Assuming a geothermal gradient of 30 °C/Km, these Th (83–115 °C) suggest a burial depth of 2100–3170 m for plagioclase albitization consistent with a Barremian–Early Aptian age or later. Thus, we interpret albitization as a mesodiagetic burial process. The minimum entrapment temperatures detected preclude a possible relationship between albitization of the eastern sector of the Tera Group and the hydrothermal metamorphism of the Cameros Basin. In addition, albitization occurs in all sections of the eastern sector of DS 2, not only in the areas affected by metamorphism (Fig. 1).

Table 2
Semiquantitative percentage data for phyllosilicates detected by X-ray diffraction in the claymudstones of the eastern sector of the Tera Group (DS 2). This table is complementary to Table 1. For example: sample ESP-101 contains 94% phyllosilicates, of which 100% are illites. Magaña: Magaña Fm. Matute: Sierra de Matute Fm.

Sample	Illite	Kaolinite	Chlorite	Formations
PRA7	100	0	0	Magaña (DS 2)
ALMA3	100	0	0	Magaña (DS 2)
ALMA6	100	0	0	Magaña (DS 2)
ALMA8	73	0	27	Magaña (DS 2)
ALMA12	67	0	33	Magaña (DS 2)
ALMA15	86	0	14	Magaña (DS 2)
ARZA2	100	0	0	Matute (DS 2)
ARZA4	84	0	16	Matute (DS 2)
ARZA8	69	0	31	Matute (DS 2)
3SAN10	76	0	24	Magaña (DS 2)
3SAN11	68	0	32	Magaña (DS 2)
3SAN41	78	0	22	Matute (DS 2)
ESP101	100	0	0	Ágreda (DS 1)
ESP102	100	0	0	Magaña (DS 2)
VUR108	100	0	0	Magaña (DS 2)

The chronology of the albitization process is difficult to constrain due to the pseudomorphic character of the albite grains. K-feldspar overgrowths are interpreted as eogenetic in origin (González-Acebrón, 2009). Albitization of the K-feldspar overgrowth over type 1 feldspar (detrital K-feldspar) may have been simultaneous to albite cement formation over types 2 and 3 (detrital plagioclases). The optical continuity of polysynthetic twining of the overgrowth and the grain in type 3 plagioclases could indicate the polysynthetic cements pre-date (Morad et al., 1990) or are simultaneous to the albitization process. Albite cements are post-dated by quartz cements (Fig. 9B) and hydrothermal veins (Fig. 9C). Hydrothermal cements infill large fractures (1–50 cm) and are thought to post-date albite cements (Fig. 9C), since these hydrothermal veins precipitated over the albite cements. Thus, albitization post-date eodiagenetic K-feldspars cements and pre-date the hydrothermal metamorphism dated as Albian–Coniacian (Casquet et al., 1992), pointing again to a mesodiagenetic process.

Finally, the mechanism of albitization is probably a dissolution and precipitation process (Boles, 1982; Morad, 1988; Saigal et al., 1988; Ramseyer et al., 1992) because the textural evidence presented in this study reveals that albitization is guided by weakness planes like grain fractures, cleavage traces and twining planes. The dissolution rate of feldspars is known to be greater at such planes due to their excess surface energy. These weak zones are conduits for the penetration of thin water films (Morad et al., 1990).

5.2. Sodium sources

On the basis of the first and final melting temperatures observed for primary fluid inclusions, the salinities of the albitization fluids are 20.15–22.44 wt.% NaCl eq. (201, 500–224, 400 ppm) according to a NaCl–H_2O model (Bodnar, 1993). These are strongly saline fluid inclusions, but not saline enough to be considered saturated with respect to halite. We hypothesize that possible sources for these concentrated brines are as residuals from evaporation, perhaps related to the alkaline lakes which developed during the end of DS 2 in the eastern sector of the basin. No halite precipitation has been deduced in these lakes, which is consistent with the fluid inclusion salinity values, which are below halite precipitation. This hypothesis agrees with the fact that only the DS 2 was affected by the albitization, because its closeness to this type of brines, and also with the higher intensity of the albitization process in the eastern sector. In addition, if we compare feldspar compositional data of DS 2 of the areas in which alkaline lakes were developed to the rest of the eastern studied sections, the sodium contents are higher in the sections with alkaline lake deposits on top ($Ab_{94.5}$>$Ab_{89.0}$, Appendixes 2 and 3, Fig. 1). Further, the lower part of DS 2 (Magaña Fm.) is more albitized than the upper part of DS 2 (Sierra de Matute Fm.), which present alkaline lakes in the southern zone. This fact indicates that the albitization process is not cogenetic with the lacustrine sedimentation, because the brines needed to percolate, evolve and reach higher depths, because albitization is more likely at greater depths and temperatures (Morad et al., 1990). This fact supports also the mesodiagenetic origin of albitization.

The presence of illite/smectite mixed-layers (Barrenechea et al., 2001) in the southern area of the basin (less affected by the metamorphism) demonstrates the transition from smectite to illite, which was completed in the rest of the study area which reached higher temperatures. Thus, transitions from sodium smectite to illite or chlorite could also have relieved Na.

In addition, the replacement of detrital sodium plagioclases by carbonate (Fig. 9A) can be another complementary source of sodium (Morad et al., 1990). Calcite cements and replacements corrode albite overgrowths (Fig. 9B) and are precipitated in the immediate vicinity of albitized plagioclase grains, and could thus be a by-product of calcium plagioclase albitization. In addition, type 1 K-feldspar is commonly pseudomorphed by carbonates (Fig. 9A). Thus, the replacement of sodium plagioclases by carbonate can be another Na source.

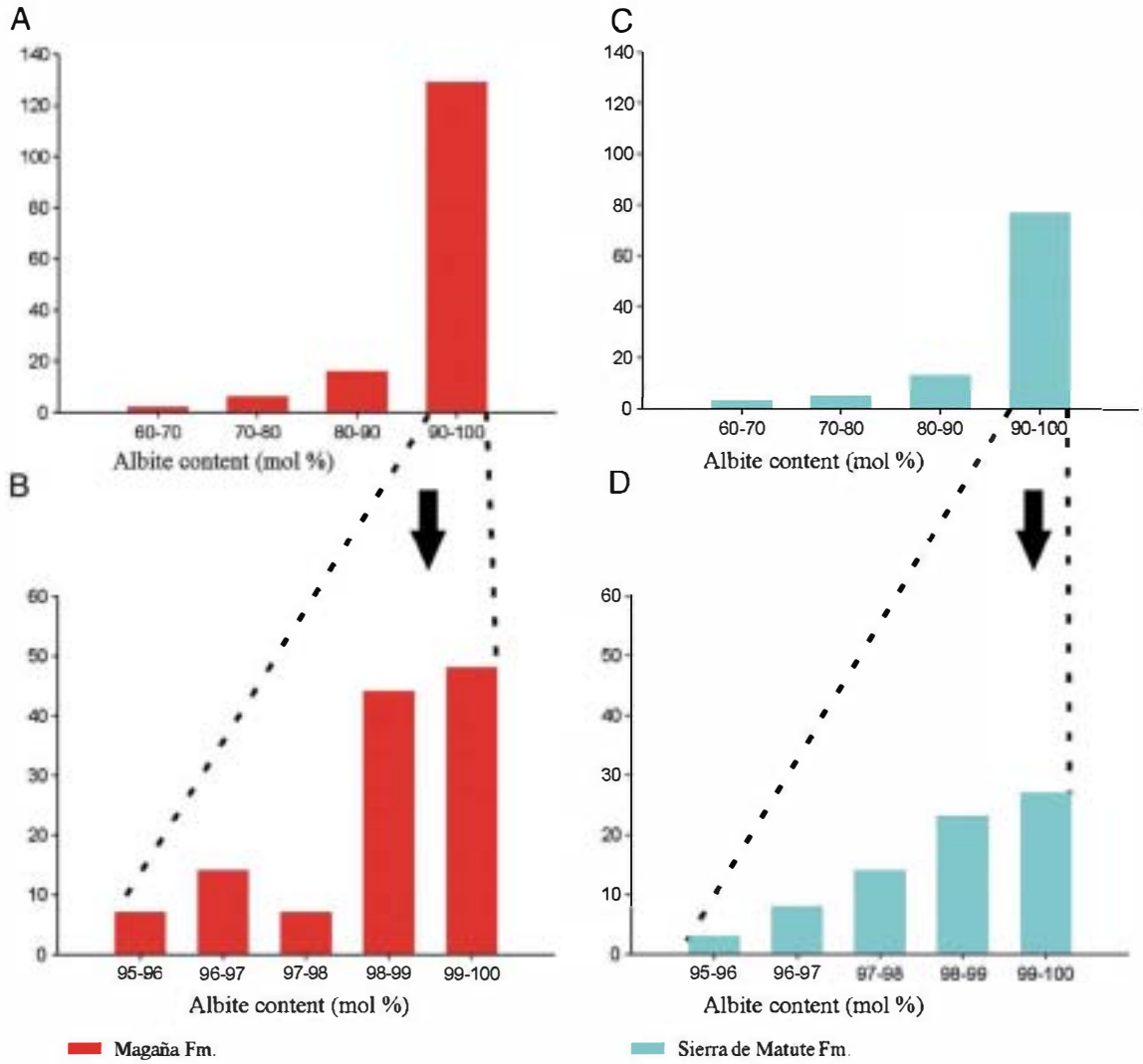

Fig. 8. Histograms showing the composition of albites in the Magaña (A and B) and Sierra de Matute Fms. (C and D). Vertical axis indicates the number of grains of albite that show a given composition in a particular interval. Histograms B or D expand the data of highly sodium-rich albites. There is a clear predominance of feldspars of albite composition (Ab: 90–100%) and very pure composition albites (Ab>99%).

6. Conclusions

Three morphological types of sodium-rich feldspars are here identified in the rifting start stage of the Cameros Basin: untwinned turbid feldspars (type 1), untwinned bright rectangular plagioclases (type 2) and polysynthetic twinned plagioclases (type 3). Types 2 and 3 appear at the top of the zone corresponding to the start of rifting.

Our petrographic evidence including cathodoluminescence and microprobe analysis, suggests a diagenetic albitization process. Albitization occurs in the upper part of the start of the rift record, affecting both plagioclases and K-feldspars. Type 1 feldspar is interpreted as detrital K-feldspar and types 2 and 3 as detrital plagioclases. Albitization post-dated K-feldspar cements and predated calcite cements, which probably represent a by-product of albitization. This albitization is interpreted here as a mesodiagenetic process, which probably occurred at burial depths of 2100–3170 m during the Barremian–Early Aptian, on the basis of the homogenization temperatures of primary fluid inclusions (83–115 °C). The lower part of the rift record has not suffered this albitization process and features very low plagioclase contents. We therefore consider albitization as a diagenetic process but provenance-related on the basis of a greater influence of plutonic and metamorphic source areas and a change in plutonic source rock composition observed towards the upper part of the record. These changes in source areas probably provided detrital plagioclases to the sandstones and the interlayered mudstones. Possible sources of Na brines are residuals from evaporation, perhaps related to the alkaline lakes which developed during the end of DS 2, clay mineral reactions (sodium smectite to illite and chlorite) and the replacement of detrital sodium plagioclases by carbonate.

Acknowledgements

Funding for this research was provided by the Spanish DIGICYT project CGL 2005-07445-CO3-02/BTE CGL2008-01648/BTE, and by UCM-CM (Universidad Complutense-Madrid Community) for the Research Group "Sedimentary Basin Analysis". The authors would like to thank the staff of the Electron Microscope Centre Luis Bru of the Complutense University (Madrid, Spain) for their help with the microprobe analyses. Sadoon Morad and Robert H. Goldstein are thanked for their useful comments and suggestions.

Appendix A. Supplementary data

Supplementary data associated with this article can be found, in the online version, at doi:10.1016/j.sedgeo.2010.06.005.

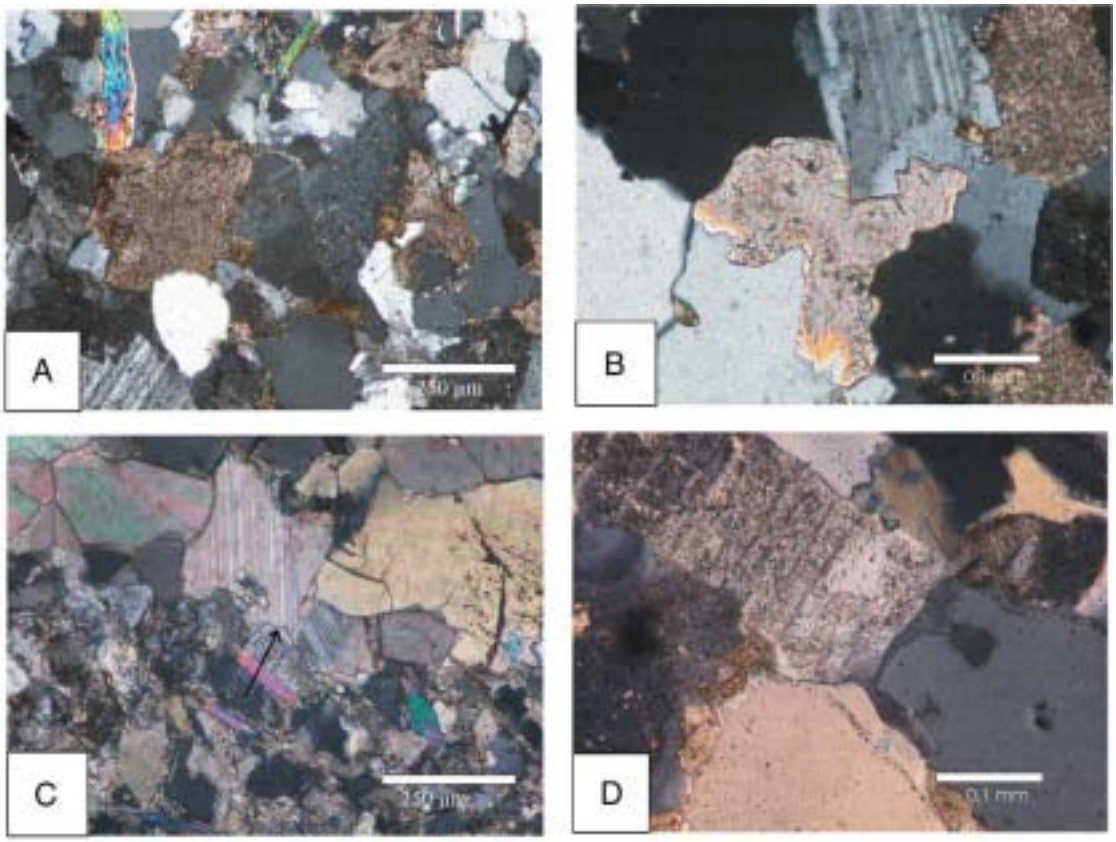

Fig. 9. Photomicrographs of feldspars in the Tera Group (crossed nichols): A. Carbonate pseudomorphic replacement of an albitized feldspar. B. The calcite cement follows the plagioclase cement, which is corroded by the calcite cement. C. Ferroan calcite cement that corrodes the albite cement of an albitized type 2 feldspar (see arrow). D. The quartz cement is prior to the albite cement and corroded by it.

References

Aagaard, P., Egeberg, P.K., Saigal, G.C., Morad, S., Bjorlykke, K., 1990. Diagenetic albitization of detrital K-feldspar in Jurassic, Lower Cretaceous and Tertiary clastic reservoir rocks from offshore Norway. II. Formation water chemistry and kinetic considerations. Journal of Sedimentary Petrology 60, 575–581.

Arribas, J., Alonso, A., Mas, R., Tortosa, A., Rodas, M., Barrenechea, J.F., Alonso-Azcárate, J., Artigas, R., 2003. Sandstone petrography of continental depositional sequences of a intraplate rift basin: Western Cameros Basin (North Spain). Journal of Sedimentary Research 73 (2), 309–327.

Arribas, J., Ochoa, M., Mas, R., Arribas, M.E., González-Acebrón, L., 2007. Sandstone petrofacies in the Northwestern sector of the Iberian Basin. Journal of Iberian Geology 33 (2), 191–206.

Barrenechea, F.J., Rodas, M., Mas, J.R., 1995. Clay mineral variation associated to diagenesis and low grade metamorphism of early Cretaceous sediments in the Cameros Basin, Spain. Clay Minerals 30, 89–103.

Barrenechea, F.J., Rodas, M., Frey, M., Mas, J.R., 2001. Clay diagenesis and low-grade metamorphism of Tithonian and Berriasian sediments in the Cameros Basin (Spain). Clay Minerals 36, 325–333.

Bodnar, R.J., 1993. Revised equation and table for determining the freezing point depression of H2O–NaCl solutions. Geochimica et Cosmochimica Acta 57, 683–684.

Boles, J.R., 1982. Active albitization of plagioclase. Gulf Coast, Tertiary. American Journal of Science 282, 165–180.

Caja, M.A., 2004. Procedencia y diagénesis de los sedimentos del Jurásico Superior–Cretácico Inferior (Facies Weald) en las subcuencas occidentales de la cuenca del Maestrazgo, Cordillera Ibérica Oriental. Ph.D. Thesis, UCM, 293 pp.

Casquet, C., Galindo, C., González-Casado, J.M., Alonso, A., Mas, R., Rodas, M., García, E., Barrenechea, J.F., 1992. El metamorfismo en la Cuenca de Los Cameros. Geocronología e implicaciones tectónicas. Geogaceta 11, 22–25.

Chayes, F., 1952. Notes of the staining of potash feldspar with sodium cobaltinitrite in thin section. American Mineralogist 37, 337–340.

Evans, A.L., 1990. Miocene sandstone provenance relations in the Gulf of Suez: Insights into Synrift Unroofing and Uplift History. American Association of Petroleum Geologists Bulletin 74, 1386–1400.

Garzanti, E., Vezzoli, G., Andò, S., Castiglioni, G., 2001. Petrology of rifted-margin sand (Red Sea and Gulf of Aden, Yemen). Journal of Geology 109, 277–297.

Garzanti, E., Andò, S., Vezzoli, G., Dell'Era, D., 2003. From rifted margins to foreland basins: investigating provenance and sediment dispersal across desert Arabia (Oman, U.A.E.). Journal of Sedimentary Research 73 (4), 572–588.

Gold, P.B., 1987. Textures and geochemistry of authigenic albite from Miocene sandstones, Lousiana Gulf Coast. Journal of Sedimentary Petrology 57, 353–362.

Goldstein, R.H., Reynolds, T.J., 1994. Systematics of fluid inclusions in diagenetic minerals. : SEMP Short course, 31. 192 pp.

Gómez Fernández, J.C., Meléndez, N., 1994. Estratigrafía de la Cuenca de los Cameros (Cordillera Ibérica Noroccidental, N de España) durante el tránsito Jurásico–Cretácico. Revista Sociedad Geologica de España 7 (1–2), 121–139.

González-Acebrón, L., 2009. El Grupo Tera en el Sector Oriental de la Cuenca de Cameros: ambientes sedimentarios, procedencia y evolución diagenética. The Tera group in the Eastern Sector of the Cameros Basin: sedimentary environments, provenance and diagenetic evolution. European Ph.D. Thesis. 422 pp.

González-Acebrón, L., Arribas, J., Mas, R., 2007a. Provenance of fluvial sandstones at the start of late Jurassic–early Cretaceous rifting in the Cameros Basin (N. Spain). Sedimentary Geology 202, 138–157.

González-Acebrón, L., Mas, R., Arribas, J., Goldstein, R.H., Benito, M.I., 2007b. Multiphase quartz cementation in sandstones: Tera Gr. (Tithonian, Cameros Basin, NE Spain). 25th IAS meeting, Patras (Grecia). Book of abstracts, p. 240.

González-Acebrón, L., Arribas, J., Mas, R., 2010. Sand provenance and implications for paleodrainage in a rift basin: the Tera Group. Journal of Iberian Geology 36 (1), 179–184.

Guimerà, J., Alonso, A., Mas, R., 1995. Inversion of an extensional-ramp basin by a newly formed thrust: the Cameros Basin (N Spain). In: Buchanan, J.G., Buchanan, P.G. (Eds.), Basin Inversion: Geological Society Spec. Publ. 88, pp. 433–453.

Hurlbut, J.R., Klein, C., 1990. Manual de mineralogía de Dana. Tercera edición. 564 pp. Ed. Reverté.

Kastner, M., 1971. Authigenic feldspars in carbonate rocks. American Mineralogists 56, 1403–1442.

Martín Closas, C., Alonso Millán, A., 1998. Estratigrafía y Bioestratigrafía (Charophyta) del Cretácico Inferior en el sector occidental de la Cuenca de Cameros (Cordillera Ibérica). Revista de la Sociedad Geológica de España 11, 253–269.

Mas, J.R., Alonso, A., Guimerà, J., 1993. Evolución tectonosedimentaria de una cuenca extensional intraplaca: la cuenca finijurásica–eocretácica de los Cameros (La Rioja-Soria). Revista de la Sociedad Geológica de España 6 (3–4), 129–144.

Mas, J.R., Benito, M.I., Arribas, J., Serrano, A., Guimerà, J., Alonso, A., Alonso-Azcárate, J., 2002. La Cuenca de Cameros: desde la extensión finijurásica–eocretácica a la inversión terciaria—implicaciones en la exploración de hidrocarburos. Instituto de Estudios Riojanos, Zubía, p. 14.

Mas, J.R., Benito, M.I., Arribas, J., Serrano, A., Guimerà, J., Alonso, A., Alonso-Azcárate, J., 2003. The Cameros Basin: from late Jurassic–Early Cretaceous Extension to Tertiary contractional inversion-implications of hydrocarbon exploration. AAPG International Conference and Exhibition, Barcelona, Spain. Geological Field Trip 11.

Mas, J.R., (Coord.), GARCÍA, A., (Coord.), Salas, R., Meléndez, A., Alonso, A., Aurell, M., Bádenas, B., Benito, M.I., Carenas, B., García-Hidalgo, J.F., Gil, J., Segura, M., 2004. 5.3.3. Segunda fase

de rifting: Jurásico Superior–Cretácico Inferior. In: Vera, J. (Ed.), Geología de España. Sociedad Geológica de España—Instituto Geológico y Minero de España, pp. 503–509.
McBride, E., 1985. Diagenetic processes that affect provenance determination in sandstones. In: Zuffa, G.G. (Ed.), Provenance of arenites: NATO ASI Series, C-148, pp. 95–113.
Milliken, K.L., 2005. Late diagenesis and mass transfer in sandstone-shale sequences. In: Mackenzie, F.T. (Ed.), Treatise on geochemistry 7: Sediments, diagenesis and sedimentary rocks.
Morad, S., 1988. Albitized microcline grains of post-depositional and probable detrital origins in Brøtum Formation sandstones (Upper Proterozoic), Sparagmite Region of Southern Norway. Geological Magazine 125, 229–239.
Morad, S., Bergan, M., Knarud, R., Nystuen, J.P., 1990. Albitization of detrital plagioclase in Triassic Reservoir sandstones from the Snorre Field, Norwegian North Sea. Journal of Sedimentary Petrology 60 (3), 411–425.
Morad, S., Ketzer, J.M., De Ros, F., 2000. Spatial and temporal distribution of diagenetic alterations in siliciclastic rocks: implications for mass transfer in sedimentary basins. Sedimentology 47, 95–120.
Ochoa, M., 2006. Procedencia y diagénesis del registro arenoso del Grupo Urbión (Cretácico inferior) en la Cuenca de Cameros (Cordillera Ibérica septentrional). 240 pp.
Ramseyer, K., Boles, J.R., Lichtner, P.C., 1992. Mechanism of plagioclase albitization. Journal of Sedimentary Petrology 62 (3), 349–356.
Saigal, G.C., Morad, S., Bj rlykke, K., Egeberg, P.K., Aagaard, P., 1988. Diagenetic albitization of detrital K-feldspar in Jurassic, Lower Cretaceous, and Tertiary clastic reservoir rocks from offshore Norway, I. Textures and origin. Journal of Sedimentary Petrology 58 (6), 3–13.
Salas, R., Guimerá, J., Mas, J.R., Martín-Closas, C., Meléndez, A., Alonso, A., 2001. Evolution of the Mesozoic Central Iberian Rift System and its Cainozoic inversion (Iberian Chain). In: Cavazza, W., Roberson, A.H.F.R., Ziegler, P. (Eds.), Peri-Tethyan Rift-Wrench Basins and Passive Margins: Mém. Mus. Nat. Hist. Natur., 186, pp. 145–185.
Trevena, A.S., Nash, W.P., 1981. An electron microprobe study of detrital feldspar. Journal of Sedimentary Petrology 51 (1), 137–150.
Walker, T.R., 1984. Diagenetic albitization of potassium feldspar in arkosic sandstones. Journal of Sedimentary Petrology 54 (1), 3–16.